

INTERPRETATION OF VARIOUS  
NUCLEAR RESONANCES

BY

PAUL WASHINGTON CRUTCHFIELD, JR.

Thesis  
C923

Library  
U. S. Naval Postgraduate School  
Monterey, California









INTERPRETATION OF VARIOUS NUCLEAR RESONANCES

by

Paul Washington Crutchfield, Jr.

Date: 8 December 1955

Approved:

Harry W. Hassen

K. M. Williams

F. D. Dressel

A thesis

submitted in partial fulfillment  
of the requirements for the  
degree of Master of Arts  
in the Graduate School  
of Arts and Sciences  
of  
Duke University

1955

Thesis  
C923



#### ACKNOWLEDGMENTS

I wish to express my appreciation to Professor Henry M. Newsen, who suggested this topic and gave me invaluable counsel and guidance in the experimental work, its analysis, and in the preparation of this thesis. I would also like to thank the other members of the Van de Graaff group at Duke University, particularly Dr. Harvey Marshak, Dr. Willy Haeberli, and Dr. Robert C. Block for their assistance.

My pursuit of studies at Duke University is under the auspices of the U. S. Naval Postgraduate School at Monterey, California, and the Office of Naval Research.

Paul Washington Crutchfield, Jr.  
Lieutenant Commander, U. S. Navy



# TABLE OF CONTENTS

	Page
ACKNOWLEDGMENTS . . . . .	1
Chapter	
I INTRODUCTION . . . . .	2
II DESCRIPTION OF EXPERIMENTAL APPARATUS . . . . .	6
III METHODS OF ANALYSIS . . . . .	13
IV PROCEDURE . . . . .	21
V THE 3 KEV RESONANCE OF SODIUM . . . . .	23
VI THE 53 KEV RESONANCE OF SODIUM . . . . .	31
VII THE FLUORINE RESONANCES AT 27 KEV, 49 KEV, AND 100 KEV . . . . .	38
BIBLIOGRAPHY . . . . .	47



# LIST OF FIGURES

	Page
1 OVERALL VIEW OF EXPERIMENTAL APPARATUS . .	10
2 VIEW OF WATER TANK . . . . .	11
3 VIEW OF SAMPLE HOLDER . . . . .	12
4 A THEORETICAL TOTAL CROSS SECTION CURVE OF THE 3 KEV SODIUM RESONANCE WITH $\ell=0$ NEUTRONS, $J=1$ , $r=0.40$ KEV, AND $\sigma_{pot}=4.8$ BARNS . . . . .	29
5 EMPIRICAL FIT OF 3 KEV SODIUM RESONANCE ASSUMING $\ell=1$ NEUTRONS . . . . .	30



## INTERPRETATION OF VARIATIONAL MODELS IN RESONANCE





## Chapter I

### INTRODUCTION

It is obviously impossible to make direct observations of nuclear particles because of their extremely small dimensions, but many experimental methods for studying these particles are available to the world of physics. Although these methods provide only indirect information, they do afford numerous opportunities both to develop and to confirm theories purporting to explain the nature of nuclear properties. The study of nuclear cross sections is one such line of attack.

If a thin sample of a given element of thickness  $\Delta v$  measured in number of atoms per unit area is interposed into the path of a beam of neutrons, the number of neutrons that will be deflected from their paths will be proportional to the number of incident neutrons,  $N$ , and the thickness of the sample,  $\Delta v$ . Hence  $\Delta N = (-)N\sigma_t\Delta v$ , where  $\sigma_t$  is a proportionality factor called the total cross section. Its units are area per atom. With the use of standard differential equation techniques, it can be shown easily that  $\sigma_t = (1/v)\ln (N_0/N_v)$  where  $N_0$  is the number of neutrons incident upon the sample, and  $N_v$  is the attenuated number of undeflected neutrons at thickness  $v$ . The experimental measurements of cross sections in support of this

# THEORY

## 1. INTRODUCTION

The first part of the paper is devoted to the study of the properties of the function  $f(x)$  defined by the equation  $f(x) = \int_0^x f(t) dt$ . It is shown that  $f(x)$  is a constant function, and its value is determined by the initial condition  $f(0) = 1$ . The second part of the paper is devoted to the study of the properties of the function  $g(x)$  defined by the equation  $g(x) = \int_0^x g(t) dt$ . It is shown that  $g(x)$  is a constant function, and its value is determined by the initial condition  $g(0) = 1$ .

The third part of the paper is devoted to the study of the properties of the function  $h(x)$  defined by the equation  $h(x) = \int_0^x h(t) dt$ . It is shown that  $h(x)$  is a constant function, and its value is determined by the initial condition  $h(0) = 1$ . The fourth part of the paper is devoted to the study of the properties of the function  $k(x)$  defined by the equation  $k(x) = \int_0^x k(t) dt$ . It is shown that  $k(x)$  is a constant function, and its value is determined by the initial condition  $k(0) = 1$ . The fifth part of the paper is devoted to the study of the properties of the function  $l(x)$  defined by the equation  $l(x) = \int_0^x l(t) dt$ . It is shown that  $l(x)$  is a constant function, and its value is determined by the initial condition  $l(0) = 1$ . The sixth part of the paper is devoted to the study of the properties of the function  $m(x)$  defined by the equation  $m(x) = \int_0^x m(t) dt$ . It is shown that  $m(x)$  is a constant function, and its value is determined by the initial condition  $m(0) = 1$ . The seventh part of the paper is devoted to the study of the properties of the function  $n(x)$  defined by the equation  $n(x) = \int_0^x n(t) dt$ . It is shown that  $n(x)$  is a constant function, and its value is determined by the initial condition  $n(0) = 1$ . The eighth part of the paper is devoted to the study of the properties of the function  $o(x)$  defined by the equation  $o(x) = \int_0^x o(t) dt$ . It is shown that  $o(x)$  is a constant function, and its value is determined by the initial condition  $o(0) = 1$ . The ninth part of the paper is devoted to the study of the properties of the function  $p(x)$  defined by the equation  $p(x) = \int_0^x p(t) dt$ . It is shown that  $p(x)$  is a constant function, and its value is determined by the initial condition  $p(0) = 1$ . The tenth part of the paper is devoted to the study of the properties of the function  $q(x)$  defined by the equation  $q(x) = \int_0^x q(t) dt$ . It is shown that  $q(x)$  is a constant function, and its value is determined by the initial condition  $q(0) = 1$ .

thesis were accomplished by inserting samples of the element (or compound) of interest into the path of a collimated beam of neutrons. Comparison of the count of neutrons with no sample inserted,  $N_0$ , with the count when a sample of thickness  $v$  was inserted, yielding  $N_v$ , provides, by means of the above formula, an experimental value of the total cross section,  $\sigma_t$ .

Slatt and Weisskopf define the cross section of a reaction (1):\*

$$\sigma = \frac{\text{Number of events of a given type/unit time/nucleus}}{\text{Number of incident particles/unit area/unit time}} \quad (1)$$

This  $\sigma$  is clearly proportional to the probability of the given type of event taking place, and  $\sigma_t$  is proportional to the sum of the probabilities of all the possible nuclear events. Many different events are possible; among them are elastic scattering of neutrons, inelastic scattering of neutrons, and capture of neutrons. The cross sections measured herein were actually total cross sections, but in the energy regions observed elastic scattering of neutrons was the overwhelmingly predominant event.

When the value of  $\sigma_t$  is measured for various energies of incident neutrons, peaks in the cross section curve are observed. These peaks (and valleys in some cases) are called resonances. Their existence is not anticipated from any theory of classical mechanics. By the methods of wave or quantum

---

\*Reference numbers in parentheses refer to numbered references in the bibliography.





mechanics, Breit and Wigner have explained the occurrence of such resonances (2). The resonances occur in the case of elastic scattering of neutrons when the energy of the compound nucleus (original nucleus plus incoming neutron) corresponds to a discrete quantum state.

The basic equations of the Breit-Wigner one-level formula are:

$$\sigma_{\text{res}} = 4\pi\lambda^2 \frac{\left(\frac{\Gamma}{2}\right)^2 \cos 2kh}{(E - E_0)^2 + \left(\frac{\Gamma}{2}\right)^2} \quad (2)$$

$$\sigma_{\text{int}} = 4\pi\lambda^2 \frac{(E - E_0) \frac{\Gamma}{2} \sin 2kh}{(E - E_0)^2 + \left(\frac{\Gamma}{2}\right)^2} \quad (3)$$

$$\sigma_{\text{pot}} = 4\pi\lambda^2 \sin^2 kh \approx 4\pi R^2 \quad (4)$$

$$\sigma_t = \sigma_{\text{res}} + \sigma_{\text{int}} + \sigma_{\text{pot}} \quad (5)$$

where  $\sigma_{\text{res}}$  is the resonance cross section term,  $\sigma_{\text{pot}}$  is approximately the cross section which would be observed if the actual nucleus were replaced by an impenetrable sphere of radius  $R$ , and  $\sigma_{\text{int}}$  is an interference term resulting from the wave properties of the neutron.  $\lambda$  is the Dirac wave length of the incoming neutron,  $k$  is the wave number of the incoming neutron,  $E$  is the energy of the incoming neutron,  $E_0$  is the resonant energy,  $\Gamma$  is the width of the resonance at one-half of  $\sigma_0$ , the



maximum value of the resonance, and  $g$  is a statistical factor,  $g = (2J + 1)/(2I + 1)(2s + 1)$ ,  $J$  is the total angular momentum quantum number of the compound nucleus,  $I$  is the spin of the target nucleus, and  $s$  is the spin of the neutron ( $1/2$ ).

There is no known theory which will predict the energies ( $E_0$ ), widths ( $\Gamma$ ), or quantum numbers ( $J$ ) of the compound states of any nucleus. Efforts to calculate average level spacings have so far yielded only qualitative success. The complex potential model (3) predicts the ratio of the average spacing to the average width. The Breit-Wigner theory provides the basis for determining the quantum numbers and widths from observed cross section curves when well separated resonances are observed.

In these experiments protons (accelerated by the 4 Mev Van de Graaff accelerator at Duke University) bombarded a lithium target. The reaction which occurs above a threshold of 1822 kev of proton energy in the laboratory system, produces neutrons and beryllium ( $Be^7$ ). With the apparatus used in these experiments the average energy spread of neutrons so obtained was reasonably small (of the order of 1 kev). The exact character of the energy distribution, however, was unknown. Nevertheless, it is possible to make some reasonable assumptions in regard to energy distribution which simplify analysis of experimental data. In general, action taken to decrease the energy spread of the neutron beam tends to decrease the intensity of the beam. A compromise is therefore necessary between beam intensity and energy homogeneity.





The principle objective in these experiments and their analyses has been to overcome the lack of knowledge of neutron energy spread and analyze the 3 kev and the 53 kev resonances in sodium and the 27 kev, the 49 kev, and 100 kev resonances of fluorine by means of transmission experiments in order to determine the quantum numbers of the states associated with the resonances and in order to determine the widths ( $\Gamma$ ) of the resonances.



## Chapter II

### DESCRIPTION OF EXPERIMENTAL APPARATUS

The apparatus used consisted of a Van de Graaff Electrostatic Generator, a magnetic analyzer, a cylindrical electrostatic analyzer, a lithium target, a Melsyn operated sample holder, a water-filled tank with a neutron collimating cavity, and boron trifluoride ( $\text{BF}_3$ ) counters. Figure 1 shows an overall picture of the experimental apparatus; Figure 2 shows the water tank; and Figure 3 shows the sample holder.

The output of the Van de Graaff accelerator consisted of hydrogen ions (protons), ionized hydrogen molecules, and impurities. The first selection in regard to type of particle was accomplished by a magnetic analyzer which deflected the proton beam  $18^\circ$  in the horizontal plane and separated protons from other particles which were deflected by angles considerably less than  $18^\circ$ . The strength of the proton beam in this segment of the apparatus was about 25 to 50 microamperes.

Principal energy analysis was accomplished in the electrostatic analyzer which deflected the proton beam through an additional horizontal angle of  $90^\circ$ . By this means energy resolution was improved to the order of 0.05%, but beam strength was reduced to a few microamperes.





Protons emerging from the electrostatic analyzer bombarded a thin lithium target. The target was prepared by soldering platinum foil, which was two mils thick, to one end of a silver tube. Platinum and silver were used because their resonances are quite narrow and their use produces uniform and generally negligible effects on the experiments. A flange was soldered to the other end of the tube. The tube, which was three inches in length and three-quarters of an inch in diameter, was made of tubing of 9 mils in thickness. The target tube was positioned in an evacuated bell jar, and lithium was heated by electricity and evaporated onto the inner side of the platinum end plate. A brass shim stock liner was temporarily inserted during the evaporation process to avoid coating the sides of the tube with lithium. Upon removal of the target from the bell jar, its flange was bolted to the end of the proton beam collimating tube as rapidly as possible and immediately put under vacuum. A charcoal trap cooled by liquid air was used near the lithium target to improve the vacuum and help maintain the target's purity.

The thickness of the lithium coating was a compromise between neutron yield and neutron energy spread. An arbitrary standard thickness of bismuth was used to test the target for lithium coating thickness and neutron yield. A transmission ratio of about 50% at the 12 kev resonance of bismuth with a neutron counting rate of about 3000 per minute was determined by experience to be a good criterion for target acceptance.



The samples of the various substances studied were mounted on a spoke-like sample holding device which was remotely controlled at the control panel by relays (see Figure 3). This arrangement was used for reasons of safety and economy of time. The neutron flux in the vicinity of the target and the samples predicated a remote control system in order to avoid over-exposure of experimenters to radiation. The spoke-like arrangement permitted the simultaneous study of several thicknesses of the same material or several different substances at each energy. An indicator light at the control panel showed which sample was in place for a run. The sample holder was mounted in such a manner that the sample, when in place, lay between the proton focal point on the lithium target and the neutron counting device.

A water tank shield was used to limit the angles through which neutrons were accepted for counting; this limited the neutron energy spread for a given proton energy. The water tank was so constructed that neutrons were accepted between  $121^\circ$  and  $123^\circ$  in the vertical plane measured from the proton beam path and  $10^\circ$  in traverse to each side. A means of determining neutron energy was thus effected, since, for a given proton energy in the laboratory system, neutron energy is a function of this angle in the vertical plane. The purpose of the water surrounding this opening was to degrade and capture neutrons at improper angles and prevent such neutrons from being counted.

A matrix of boron trifluoride ( $\text{BF}_3$ ) counters imbedded in





paraffin was placed at the bottom of this tank cellulating tube. The counters were arranged in such manner that the probability of counting neutrons which entered the counter was maximized.  $\text{BF}_3$  counters work most efficiently with thermalized neutrons. Paraffin served the purpose of thermalizing the high energy neutrons entering the matrix. For more details concerning the counting matrix and the water tank, see the Ph.D. thesis of Dr. John H. Gibbons (4).

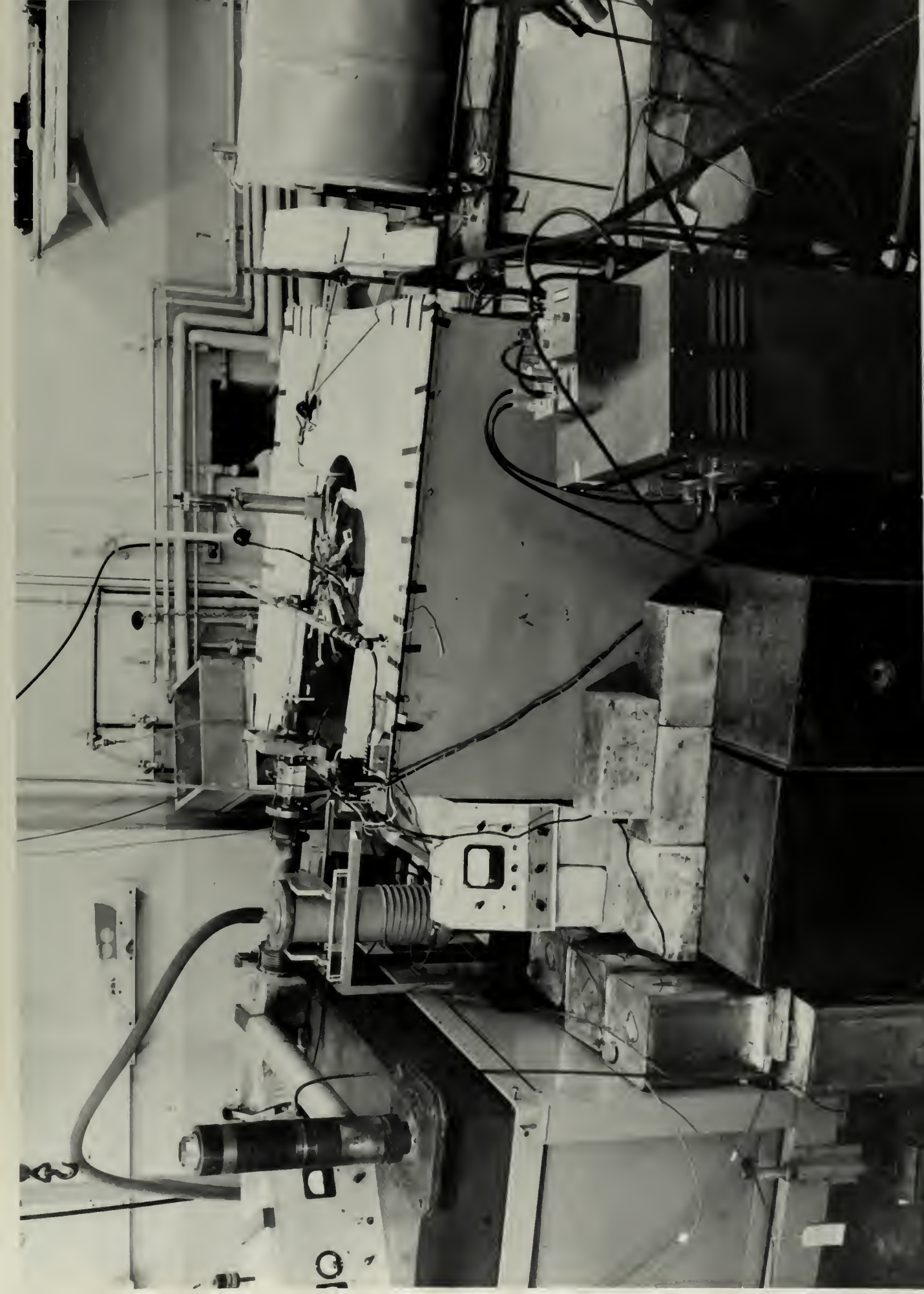




Figure 1















### Chapter III

#### METHODS OF ANALYSIS

The equation for the total cross section developed in Chapter I,  $\sigma_t = (1/v) \ln (N_0/N_v)$ , where  $\sigma_t$  is the total cross section,  $v$  is the target thickness,  $N_0$  is the number of neutrons entering the sample, and  $N_v$  is the attenuated number of neutrons at thickness  $v$ , is valid for the case where monoenergetic neutrons are used, or where  $\sigma_t$  is independent of neutron energy. The actual cross section observed in transmission experiments is a weighted average value of the cross sections for the different energy values of the incoming neutrons. For purposes of clarification,  $\sigma_{app}$  is defined  $\sigma_{app} = (1/v) \ln (N_0/N_v)$ , where  $N_0$  is the experimentally observed "sample out" count corrected for background, and  $N_v$  is the "sample in" count corrected for background and potential scattering.

A continuing effort is exerted in all measurements of cross sections to reduce the energy spread of the incoming neutrons, but some spread always exists. If the spread is small in comparison with the width of a resonance, the measured peak cross section value is almost equal to the true peak cross section value. If the spread is large in comparison with the width of the resonance, the measured peak cross section value is



considerably less than the true peak cross section value. In fact, a very narrow resonance might not even be detected in that its small observed peak could be attributed to statistical error.

If the true peak cross section value were uniquely determined by the energy at which a resonance occurs, a neutron energy spread narrow enough to allow mere detection of a resonance would suffice for determining the true peak cross section value. Actually several discrete values of the peak cross section are possible depending upon the total angular momentum quantum number,  $J$ , of the compound nucleus through the statistical weight factor,  $g$ , explained in Chapter I. Teichmann has shown that only a few  $J$  values are to be expected as possibilities (9). Accordingly, very good neutron energy resolution is invaluable in determining the true peak cross section value. Also, a good knowledge of the character of the neutron energy spread would facilitate evaluation of experimental data.

One approach to this situation is to consider the neutrons that are scattered as the beam passes through successive layers or thicknesses of a substance. In the case of a normal or Gaussian energy distribution of neutrons with average energy corresponding to that of the peak of the resonance, the probability of being scattered is lower on the wings of the Gaussian curve (away from the resonant energy) than it is near the center of the Gaussian curve (near the resonant energy). Hence, with an incoming Gaussian energy distribution, the neutrons scattered in thickness  $v$  of the substance have an energy





distribution which is leptokurtic, or more peaked than a Gaussian. The degree of kurtosis of this distribution is also smaller than that of the resonance curve itself, indicating that the energy distribution curve of the scattered neutrons is more peaked than the resonance curve. The unscattered neutrons at thickness  $v$  would have a platykurtic, or broader than Gaussian, energy distribution. The degree of kurtosis of the energy distribution of neutrons between thickness  $v$  and thickness  $2v$  would be smaller than that of the energy distribution of neutrons unscattered at thickness  $v$ . Determination of the cross section by the formula defining  $\sigma_{app}$  in the first paragraph of this chapter uses  $N_v$ , the unscattered neutrons at thickness  $v$ , which have a platykurtic energy distribution. There is another method of determining cross sections, referred to as the difference method herein, which takes advantage of the improved resolutions of the neutrons that are scattered in successive equal thicknesses. A cross section determined on the basis of this principle is defined  $\sigma_{diff} = (1/v) \ln (N_0 - N_v / N_v - N_{2v})$ , where the subscripts refer to the thickness of sample used when the neutron count,  $N$ , is obtained. The  $N$ 's should be corrected for potential scattering before insertion into this formula, in which case the value is a cross section due to the resonance alone. In the case of monoenergetic neutrons,  $\sigma_{diff} = \sigma_{app}$ . The quantity  $N_0 - N_v$  is the number of neutrons that are scattered in the first thickness,  $v$ , of the substance; the quantity  $N_v - N_{2v}$  represents the number of neutrons that are scattered



between thickness  $v$  and thickness  $2v$ . In view of the improved resolution of these quantities, it is anticipated that  $\sigma_{\text{odiff}}$  is a closer approximation to  $\sigma_0$ , the true peak resonance cross section, than  $\sigma_{\text{app}}$  is.

Mersbacher and Chern have developed by means of numerical integration a family of curves from which  $N_v/N_0$  can be determined, assuming a Gaussian neutron energy distribution (5). The other arguments besides  $N_v/N_0$  are  $A \equiv \Gamma/2.83y$ , where  $\Gamma$  is the width of the resonance and  $y$  is the standard deviation of the neutron energy distribution, and  $B \equiv v\sigma_0$  where  $v$  is target thickness and  $\sigma_0$  is the theoretical peak value of the resonance cross section. (Mersbacher uses the Greek letters  $\alpha$  for  $A$ ,  $\beta$  for  $B$ , and  $\lambda$  for  $y$ .) The relationship  $\sigma_0 \geq \sigma_{\text{odiff}} \geq \sigma_{\text{app}}$  was tested for validity by entering Mersbacher's curves with various values of  $A$  and  $B$ . The relationship proved to be accurate except for large values of  $A$  corresponding to very good neutron energy resolution. In such cases  $\sigma_{\text{odiff}}$  fell below  $\sigma_{\text{app}}$  in value. The cause of this anomaly was not pursued, since the difference method is unnecessary with good resolution. In no case did  $\sigma_{\text{odiff}}$  exceed  $\sigma_0$ . The difference method thus offers an improved approximation to the true peak cross section value. The primary weakness of the difference method formula in its application is that the error expectation is rather large in that the numerator and denominator are differences of experimentally determined values. It is particularly sensitive to a variation in  $N_v$ .





H. A. Bethe has derived an expression for determining the peak cross section value of a resonance term,  $\sigma_0$ , by a self absorption method which can be applied even to a flat distribution of neutron energies (8). Bethe's formula applies to the situation in which a thin layer of resonant absorber or scatterer is placed into a collimated beam of neutrons and serves as a detector. A  $\beta, \gamma$  or neutron counting device may be used as a measure of the number of interacting neutrons. The transmission ratio,  $z$ , is measured by placing various thicknesses of the same material upstream from the detector layer. Bethe's formula gives this ratio,  $z = \exp(-B/2) J_0(iB/2)$ , where  $J_0$  is the Bessel function of order zero and  $B = v \sigma_0$ . The value of  $\sigma_0$  can be calculated from the value of  $B/2$  obtained from the curve, since the thickness of the absorber sample,  $v$ , is known. The method is applicable only to isolated resonances.

$N_0 - N_v$ , the numerator in the formula for  $\sigma_{\text{diff}}$ , is the number of neutrons that are scattered in thickness  $v$ , corresponding to the counts that would be observed with the detector layer alone in the beam. The difference  $N_v - N_{2v}$ , the number of neutrons scattered in the second thickness, corresponds to neutrons detected in Bethe's arrangement.

If the ratio  $N_v - N_{2v} / N_0 - N_v$  is used as  $z$  in Bethe's curve, a cross section, defined  $\sigma_{\text{ob}}$ , can be obtained. This cross section should be considerably larger than the true cross section, since Bethe's formula is based upon a flat incoming neutron energy distribution. The distribution used in these





experiments is considerably better than a flat distribution.

A cross section,  $\sigma_{ob}$ , obtained from Bethe's curve thus provides an expected upper limit to the value of the true cross section,  $\sigma_0$ . Bethe's formula is based upon a thin detector layer, therefore with thicknesses used in these experiments,  $\sigma_{ob}$  is an approximate upper limit.

With the above facts in mind, samples were prepared in single, double, and higher harmonic thicknesses. Some of the sodium cross sections were measured by using sodium fluoride (NaF) samples. Chemically pure powdered NaF crystals were heated to expel any water, weighed, and compressed in a circular die of 1-1/8 inch diameter. They were canned in brass tubing which had a wall thickness of about 1/32 inch. One mil silver sheets were soldered on each end to maintain the dryness of the samples. The samples were then glued to sample holding adapters and bolted to the sample holder above the water tank. Thicknesses of the NaF samples are given in Table I.

Table I. NaF SAMPLE THICKNESSES

Sample number	Na atoms/sq cm
1	$0.377 \times 10^{22}$
2	$0.766 \times 10^{22}$
3	$1.533 \times 10^{22}$
4	$3.027 \times 10^{22}$
5	$5.941 \times 10^{22}$





Attempts were also made to prepare phosphorus samples from red phosphorus, but apparently the samples could not be dried sufficiently for use in transmission experiments.

Fluorine samples were obtained quite simply by using single and double thicknesses of 1/8 inch teflon (polytetrafluoroethylene -  $\text{CF}_2$ ). A thickness of 1/8 inch has  $1.66 \times 10^{22}$  fluorine atoms per sq cm.

An hermetically sealed metallic sodium sample prepared by Dr. A. L. Toller for a previous experiment was also used. Its thickness was  $2.407 \times 10^{22}$  atoms per square centimeter.

The Gaussian resolution curves discussed in the description of the difference method provide the basis for a method of peak height analysis which was developed by Merzbacher and Chern (5). The three arguments to the curves are  $N_v/N_0$ , the transmission ratio,  $A \equiv \Gamma/2.83y$  where  $\Gamma$  is the width of the resonance and  $y$  is the standard deviation of the incoming neutron energy distribution, and  $B \equiv v \sigma_0$  where  $v$  is the target thickness in atoms per square centimeter and  $\sigma_0$  is the peak value of the cross section due to the resonance alone.  $N_v/N_0$  is determined experimentally. The thickness,  $v$ , can be determined with reasonably good accuracy; a few discrete values of  $\sigma_0$  can be determined, depending upon the statistical weight factor,  $g$ , described in Chapter I and the resonant energy. Hence, a few discrete values of  $B$  can be postulated. With an experimentally determined  $N_v/N_0$  ( $N_v$  should be corrected for potential scattering), a value of  $A$  can be determined from the curves for each



postulated value of  $B$ . The correct choice of  $B$  should yield the same value of  $A$  when experiments are conducted with several different sample thicknesses, other conditions being the same. Therefore, consistent values of  $A$  for different sample thicknesses is evidence of a correct assumption of  $\sigma_0$ .

In addition to the peak height analysis method just described, Merzbacher and Chern have developed a method of determining the width,  $\Gamma$ , of a resonance for resonances in this energy region (5), based on an area analysis of the transmission ratio curve. The method consists essentially of measuring the area between the transmission curve and unity over a good portion of the resonance dip. The energy segments on each side of the transmission curve minimum must be equal in order to cancel the effects of the anti-symmetric interference term in the Breit-Wigner expression (see Chapter I). The method yields a different width for each postulated peak cross section value,  $\sigma_0$ . The correct choice can be made only if the total angular momentum quantum number,  $J$ , is known.

Another method of peak height analysis based upon the assumption of a rectangular neutron energy resolution is discussed in Chapter VI.





## Chapter IV

### PROCEDURE

A beam of protons was obtained by means of the Van de Graaff Electrostatic Generator. The magnetic and electrostatic analyzers were described in Chapter I. This proton beam bombarded a lithium target to yield neutrons by the  $\text{Li}^7(\text{p},\text{n})\text{Be}^7$  reaction. Since the angle of neutron acceptance was fixed at  $122^\circ \pm 1^\circ$ , the neutron energy was principally a function of proton energy.

The first step in the procedure was to check the target thickness by means of the standard bismuth sample at the 12 kev bismuth resonance (See Chapter II). If the target was satisfactory, a check of the known 1882 kev forward threshold of the  $\text{Li}^7(\text{p},\text{n})\text{Be}^7$  reaction was then made in order to calibrate voltage settings on the electrostatic analyzer.

The procedure for obtaining data was then to set the proton energy at the necessary level to attain the desired nominal neutron energy. The number of neutrons was normalized by measuring the integrated proton current hitting the lithium target. First a count of neutrons with no sample was obtained. The amount of integrated proton current was selected to yield an "out" count of about 4000 to 10,000 in order to keep the





experimental error at about 1-2%. Next the samples were inserted by the remote control Selsyn system into the collimated neutron path and "in" counts were taken. Then another "out" count was taken as a check on stability of experimental conditions during the run at that particular energy. Inasmuch as analysis of experimental data involves comparison and use of data obtained from different sample thicknesses, it was desirable that neutron counts should be taken with each sample thickness in sequence at a given energy level in order that experimental conditions would be as nearly equal as possible for all sample thicknesses.

At or near the resonant energy, where the cross section is high, thinner samples were used in order to obtain higher counting rates when the samples were "in." Away from the resonances the cross section is small and virtually independent of neutron energy. While the use of thin samples yields high "in" counts in such regions, the transmission ratio is very nearly unity thereby increasing the statistical error (in barns) in the cross section. Accordingly, thicker samples were used away from the resonances.



## Chapter V

### THE 3 KEV RESONANCE OF SODIUM

Belove et al (6) determined experimentally that the peak cross section value of the 3 kev resonance of sodium was 555 barns. (A barn is  $10^{-24}$  square centimeters.) This value corresponds to a J quantum number of 2. The experimental data reported by Brookhaven National Laboratory (7) is consistent with a J value of 1 in that no point above 333 barns was obtained. An attempt was made to fit the experimental data with a theoretical curve using  $\sigma_0 = 333$  barns,  $l = 0$  neutrons,  $J = 1$ ,  $\Gamma = 0.40$  kev at 3 kev, and  $\sigma_{pot} = 4.6$  barns. Figure 4 shows this curve together with various experimental points. The asymmetry of this curve is explained by the presence of a sizeable interference term for  $l = 0$  neutrons. A width,  $\Gamma$ , of about 0.37 kev instead of 0.40 kev would probably yield a better fit to experimental data. While this calculated curve fits experimental data quite well, it is improbable that the resolution of the Brookhaven experimental equipment would yield experimental cross sections so close to the true peak value, which is the case if a peak value of 333 barns is assumed.

An attempt to fit experimental data with  $J = 2$ ,  $l = 0$  neutrons, and a width,  $\Gamma$ , of 0.25 kev (the width found from





area analysis by the Brookhaven group) yielded very poor results in that such a narrow width is not consistent with experimental data. A width of about 0.35 kev would be needed for curve fitting of experimental data in such a case. An area analysis by the method described in Chapter III of experimental data obtained with  $\text{K}_2\text{F}$  samples 2, 3, and 4 (see Table I) yielded an average width,  $\Gamma$ , of 0.34 kev for the postulated values of  $J = 2$  and  $\ell = 0$ . The value for the width at resonance obtained from the area method agrees very well with that obtained by direct curve fitting, and the assignment  $J = 2$ ,  $\ell = 0$  seems very satisfactory. However, in order to get a detailed fit, it was necessary to assume the unreasonably high value  $\sigma_{\text{pot}} = 7$  barns; consequently, this assignment is somewhat less satisfactory than an  $\ell = 1$  assumption.

If  $\ell = 1$  neutrons are postulated, the interference term can be neglected, but the asymmetry is then explained by the fact that the width,  $\Gamma$ , varies directly with  $E^{3/2}$ . The Breit-Wigner resonance term is then altered to the approximation:

$$\sigma_{\text{res}} = \frac{2g}{3} \frac{\Gamma_r^2 E^2 E_0^{-3}}{(E - E_0)^2 + \left(\frac{\Gamma}{2}\right)^2} \quad (6)$$

where  $\sigma_{\text{res}}$  is in barns,  $g$  is the statistical weight factor described in Chapter I,  $\Gamma_r$  is the width at the resonant energy in kev,  $\Gamma$  is the width at any energy in kev,  $E$  is the neutron energy in kev, and  $E_0$  is the resonant energy in kev.



Away from the resonant energy where  $(E - E_0)$  is large compared with  $\Gamma/2$ , the second term in the denominator can be neglected. Hence, away from the resonant energy the resonance cross section is proportional to  $1^2/(E - E_0)^2$  for  $\ell = 1$  neutrons. Figure 5 shows an empirical curve fitted to experimental data by a proportionality factor of 1.8.

Because of the uncertainty of the true peak cross section value of the 3 kev resonance of sodium, experiments were conducted with the various thicknesses of sodium fluoride described in Table I. A Gaussian peak height analysis of the resonance was made in the manner described in Chapter III.  $J$  values of 1, 2, and 3 were tested. Table II shows the "A" values obtained for each sample thickness paired with each postulated  $J$  value.  $J = 0$  was not considered, since experimental values of the peak cross section,  $\sigma_{app}$ , were greater than the theoretical value of 111 barns for  $J = 0$ . Consistency of "A" values for different thicknesses is evidence of a correctly postulated  $J$  value. The results shown in Table II favor  $J = 3$  over  $J = 2$  and  $J = 1$ , but the inconsistency for  $J = 2$  is not sufficient to rule it out.  $J = 1$  appears unlikely on the basis of this analysis in agreement with the results found by Gelove and the Brookhaven group, and with the more direct observation already discussed concerning the nearness of experimental values to 333 barns, the peak cross section value for  $J = 1$ .

Evaluation of this resonance by Bethe's self absorption method described in Chapter III was also made. An upper limit





Table II. PEAK HEIGHT ANALYSIS OF THE 3 KEV SODIUM RESONANCE,  
GAUSSIAN DISTRIBUTION

Sample thickness, Na atoms/sq cm	$A_1$	$A_2$	$A_3$
$0.377 \times 10^{22}$	0.45	0.26	0.20
$0.786 \times 10^{22}$	0.35	0.27	0.18
$1.533 \times 10^{22}$	0.33	0.22	0.18
$3.027 \times 10^{22}$	0.28	0.21	0.18

\*  $A = \Gamma / 2.35\gamma$  where  $\gamma$  is standard deviation of neutron energy distribution.

Subscripts correspond to J quantum numbers.

Consistency of A values for different sample thicknesses is evidence of correct J value.

of  $\sigma_{ob} = 827$  barns was obtained by this method;  $J = 1, 2$ , or 3 are possibilities, but  $J = 3$  has  $\sigma_0 = 778$  barns, which is closer to 827 barns than is normally expected.

If  $l = 1$  is postulated, experimental data can be adjusted for the variation of the width,  $\Gamma$ , with the energy by raising the transmission ratio,  $N_v/N_0$  with  $N_v$  corrected for potential scattering, to the power  $(E_0/E)^2$ . Widths obtained from an area analysis of these adjusted transmission ratios are tabulated in Table IIIa together with widths corresponding to the proportionality factor of 1.8 used in the empirical curve in Figure 5.

Discrepancies in the values obtained by the two methods could be due to the fact that the analyses were made with two different sets of experimental data with slightly different energy scales.





Table IIa. WIDTHS,  $\Gamma$ , OF THE 3 KEV SODIUM RESONANCE RESONANCES CORRESPONDING TO J QUANTUM NUMBERS OF 1, 2, AND 3 AND  $\ell = 1$  NEUTRONS OBTAINED BY AREA ANALYSIS AND CURVE FITTING OF EXPERIMENTAL DATA

J value	J = 1	J = 2	J = 3
$\Gamma$ by area analysis, keV	$0.35 \pm 0.04$	$0.26 \pm 0.04$	$0.22 \pm 0.03$
$\Gamma$ by empirical formula, using	$0.44 \pm 0.04$	$0.34 \pm 0.04$	$0.29 \pm 0.03$
$\sigma_{\text{res}} = \frac{1.8 \text{ Å}^2}{(E - E_0)^2}$			

Area analysis by Merzbacher-Chern method with experimental transmission ratios corrected for variation of width with neutron energy,  $\Gamma = \Gamma_r(E/E_0)^{3/2}$   
 limits in values stated because of uncertainty of  $E_0$ .

A summary of the results of experiments both by myself and by others on this resonance is given in Table III. The assignment of quantum number  $J = 2$ , in agreement with Belove et al, and angular quantum number  $\ell = 1$  seems most consistent. It is hoped that angular distribution studies will clarify remaining uncertainties.



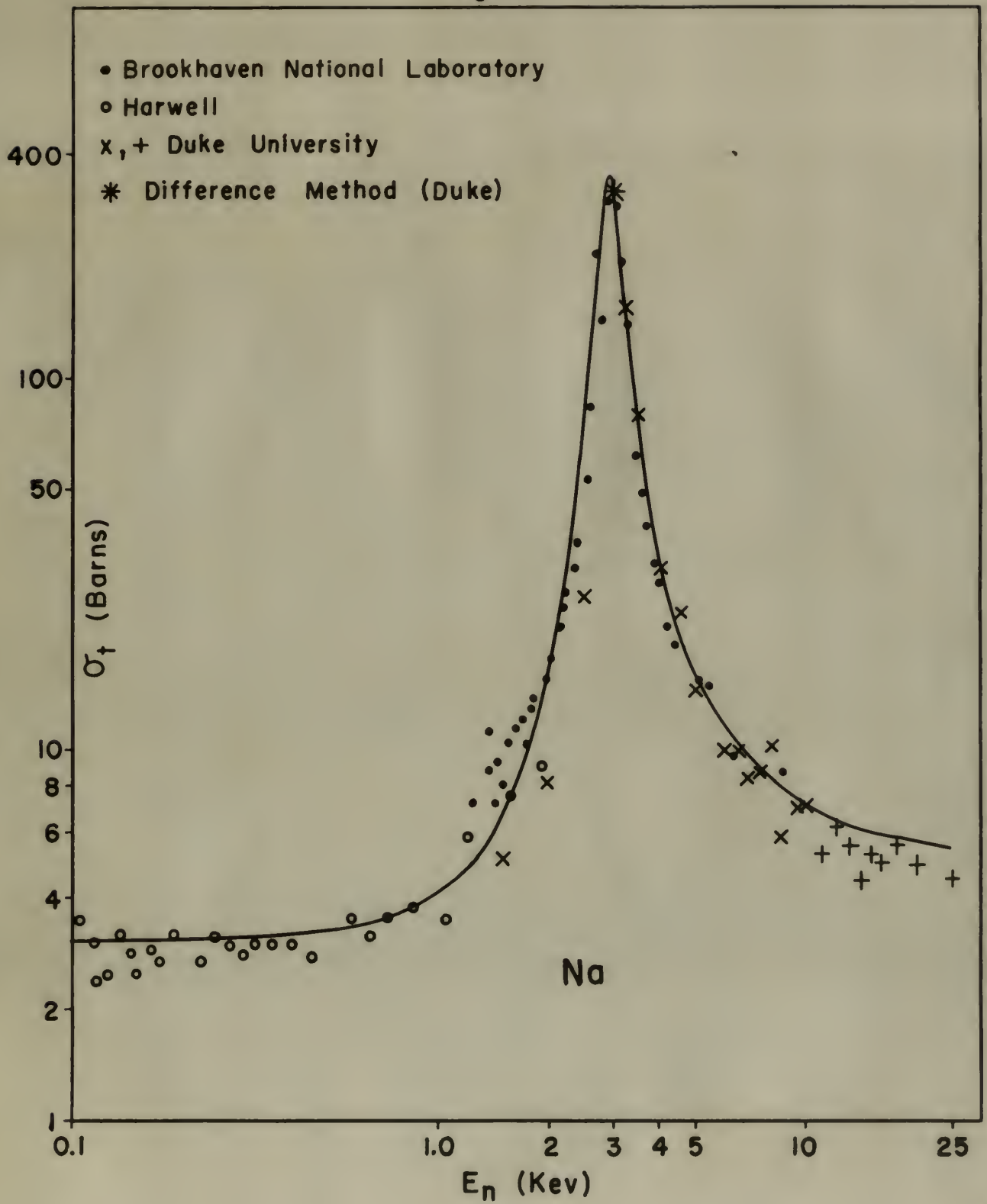
Table III. SUMMARY OF 3 KEV SODIUM RESONANCE EXPERIMENTS

J postulated	$\sigma_0$ , barns theoretical	$\ell$ assumed	Remarks
0	111	1	$\sigma_{\text{exp}}$ too high
1	333	0, 1	Consistent with shape; peak height analysis inconsistent; $\sigma_{\text{exp}}$ too high.
2	555	0, 1	Consistent with shape, peak height analysis, and $\sigma_{\text{exp}}$ .
3	778	1	Most consistent with peak height analysis
Upper limit of $\sigma_0$ ( $\sigma_{\text{ob}}$ )			827 barns
Minimum value of $\sigma_0$ - Brookhaven data			300 barns
Value of $\sigma_0$ obtained by Selove			555 barns





Figure 4





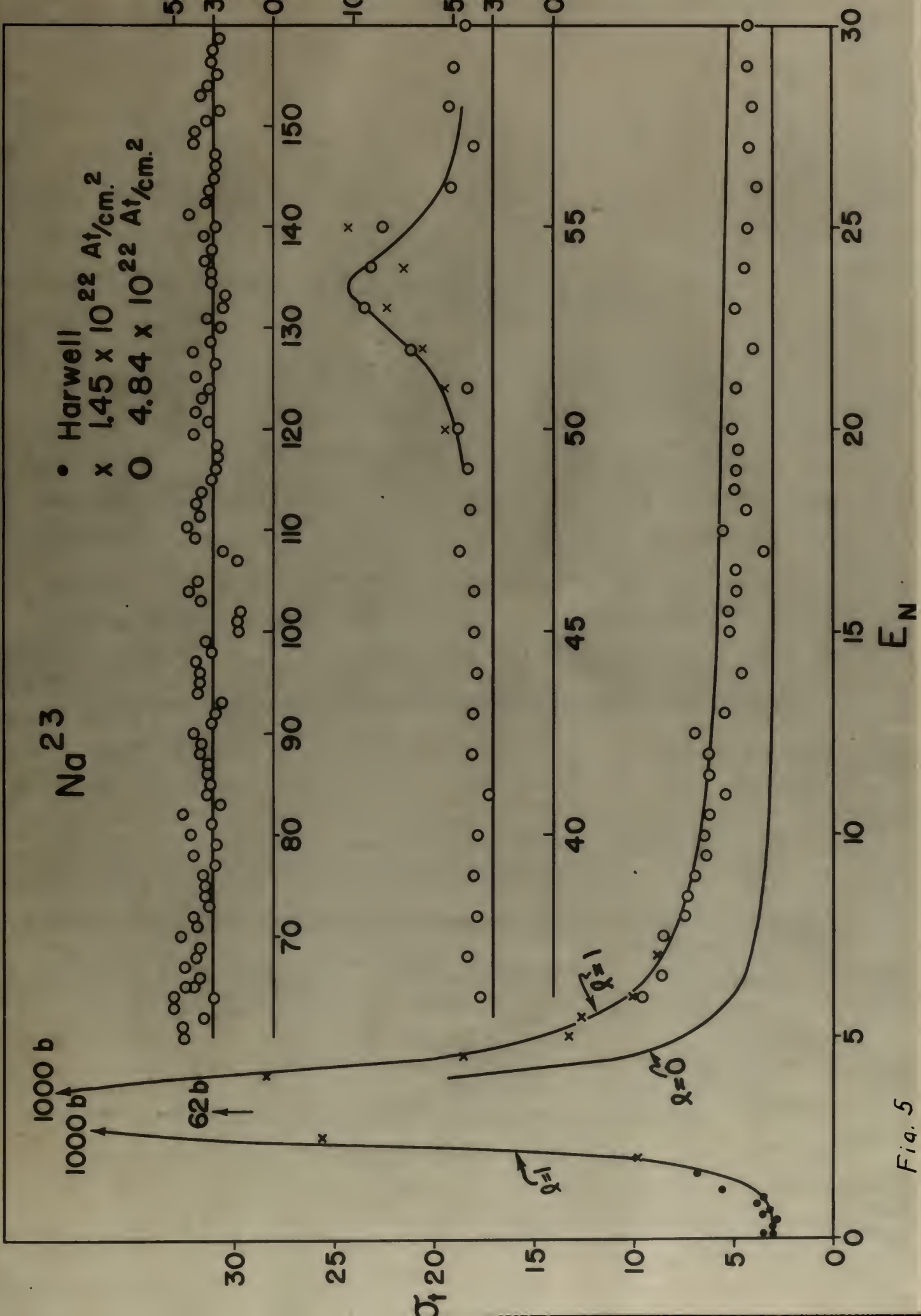


Fig. 5



## Chapter VI

### THE 53 KEV RESONANCE OF SODIUM

An area analysis of the 53 kev sodium resonance was made by the method described in Chapter III with data obtained from a neutron transmission experiment using a metallic sodium sample of thickness  $2.407 \times 10^{22}$  atoms per square centimeter. Results of this analysis are given in Table IV. The lowest value of the transmission ratio obtained with the standard bismuth sample at the 12 kev bismuth resonance peak was 0.52. This value was determined in setting up the experiment, and, in general, met the requirements of lithium target acceptability described in Chapter II.

Table IV. WIDTHS OF THE 53 KEV SODIUM RESONANCE FROM A MERZBACHER-CHERN AREA ANALYSIS

J postulated	$\sigma_{app}$ barns maximum	$\sigma_0$ barns theoretical	$\Gamma_{kev}$ calculated
1	14.2	18.9	1.70
2		31.4	1.03
3		44.0	0.78

$\sigma_{pot}$  of 3.7 barns assumed in determining  $\sigma_{app}$ .





Patterson has determined (10) that the quantum number  $J$  for this resonance should be equal to or less than 3.  $J = 0$  was not considered, since values of  $\sigma_{\text{app}}$  obtained exceeded 6.3 barns, the theoretical value of  $\sigma_0$  for  $J = 0$ .

A transmission experiment was conducted at the same time at 53 kev with NaF samples number 3, 4, and 5 (see Table I). The nearness of the 49 kev fluorine resonance complicated analysis of data obtained at 53 kev with the NaF samples. Table V shows the results of analysis of this experiment by the difference method described in Chapter III.

Table V. ANALYSIS OF 53 KEV SODIUM RESONANCE  
BY THE DIFFERENCE METHOD

$\sigma_{\text{odiff}}$	with samples 3 & 4	$\pm 1.7$ b	26.1 barns
$\sigma_{\text{odiff}}$	with samples 4 & 5	$\pm 1.0$ b	27.3 barns
$\sigma_{\text{app}}$	with sample 3 (at peak)		15.7 barns
$\sigma_{\text{app}}$	with sample 4 (at peak)		14.4 barns
$\sigma_{\text{app}}$	with sample 5 (at peak)		11.5 barns
$\sigma_{\text{pot}}$	of sodium assumed		3.7 barns
$\sigma_{\text{F}}$	of fluorine assumed		5.7 barns
$\sigma_{\text{ob}}$	upper limit, samples 3 & 4		47.0 barns
$\sigma_{\text{ob}}$	upper limit, samples 4 & 5		52.2 barns

$\sigma_{\text{ob}}$  upper limits were determined from Bethe's self-absorption curve.

Sample thicknesses are given in Table I.



Since the values of  $\sigma_{\text{diff}}$  exceed 10.9 barns, the theoretical value of  $\sigma_0$  for  $J = 1$ , the choice of  $J$  is narrowed to  $J = 2$  or  $J = 3$ . A peak height analysis, Gaussian resolution, was made by the method described in Chapter III in order to choose between  $J$  values of 2 and 3. The results of this analysis are given in Table VI.  $J = 3$  seems more consistent than  $J = 2$  in that the  $A$  values are more consistent for different target thicknesses.

Table VI. PEAK HEIGHT ANALYSIS OF THE 93 KEV SODIUM RESONANCE, GAUSSIAN RESOLUTION\*

Sample thickness, Na atoms/sq cm	$A_1$	$A_2$	$A_3$
$1.533 \times 10^{22}$	1.45	0.47	0.29
$2.407 \times 10^{22}$	1.05	0.43	0.28
$3.027 \times 10^{22}$	1.05	0.42	0.28
$5.941 \times 10^{22}$	0.70	0.38	0.28
Average value of $y$ for all thick- nesses, kev	0.57	0.85	0.98

\*  $A \equiv \Gamma / 2.83y$  where  $y$  is standard deviation of neutron energy distribution.

Subscripts correspond to  $J$  quantum numbers.

Consistency of  $A$  values for different sample thicknesses is evidence of correct  $J$  value.

Average  $y$  values based on widths tabulated in Table IV.

...and the ... ..  
 ... ..  
 ... ..  
 ... ..  
 ... ..  
 ... ..  
 ... ..  
 ... ..  
 ... ..  
 ... ..

Table 1. ... ..  
 ... ..

...	...	...	...
...	...	...	...
...	...	...	...

... ..  
 ... ..  
 ... ..  
 ... ..  
 ... ..



Another approach to the problem of correcting data for neutron energy distribution is to consider the effect of the 2 degree spread in the angular acceptance of neutrons. Even if monoenergetic neutrons were obtained from the lithium target at a particular angle, neutrons counted still have an energy spread, since neutrons are accepted for counting between 121 degrees and 123 degrees. In the case of monoenergetic neutrons leaving the lithium target in the center of mass system, the energy distribution of neutrons counted would be more or less rectangular in shape. Gibbons has calculated the energy spread as a function of neutron energy at 122 degrees for the tank arrangement used at Duke University (4). Herzog has plotted a family of curves which yield the expected transmission ratio which would be observed at a particular resonant energy with a rectangular neutron energy distribution of known energy spread. These curves may be used to calculate the expected value of the peak cross section provided  $\sigma_0$  (i.e. the total angular momentum  $J$ ), and width  $\Gamma$  are known. If the assumptions of  $\Gamma$  and  $\sigma_0$  are correct, the value of the cross section obtained by such a determination should be the maximum value obtainable with the experimental equipment at Duke University. This method of analysis can conceivably eliminate some  $J$  values for a given resonance.

A peak height analysis based upon the assumption of a rectangular neutron energy distribution was made of the 53 kev sodium resonance. Table VII shows the results of this analysis.



Table VII. PEAK HEIGHT ANALYSIS OF THE 53 KEV SODIUM RESONANCE BASED UPON  
A RECTANGULAR NEUTRON ENERGY DISTRIBUTION

Sample Number	Experi- mental $\sigma_0$	$\sigma_0$ for $\Delta E = 2.1$ kev $J = 2$	$\sigma_0$ for $\Delta E = 3.15$ kev $J = 2$	$\sigma_0$ for $\Delta E = 2.1$ kev $J = 3$	$\sigma_0$ for $\Delta E = 2.5$ kev $J = 3$	$\sigma_0$ for $\Delta E = 3$ kev $J = 3$
Diff. method 3 and 4	26.1	23.8	12.7	29.0	27.8	24.2
Diff. method 4 and 5	27.3	19.7	19.8	25.7	22.9	23.4
3	15.7	17.1	11.9	20.1	17.1	14.9
4	14.4	16.3	12.3	18.8	15.8	14.5
5	11.5	15.6	11.0	16.9	14.2	12.7

\* All values of  $\sigma_0$  are the peak values due to the resonance term alone.

$\Delta E$  obtained from Gibbon's curve (4) is 2.1 kev.

Analysis based upon widths of  $\Gamma = 1.03$  kev for  $J = 2$  and  $\Gamma = 0.78$  kev for  $J = 3$ .  
(See Table IV)





In this tabular summary, values of the peak cross section due to the resonance alone are listed. Experimental values are compared with calculated values which are obtained by correcting for a rectangular neutron energy distribution with the aid of Merzbacher's curves. The calculations were based on width values,  $\Gamma$ , from Table IV and both possible  $J$  values as indicated in Tables V and VI. The lowest value of  $\Delta E$ , width of the rectangular energy distribution in kev, which was used in the analysis was obtained from Gibbon's curve (4). Larger values of  $\Delta E$  were also used, for Gibbon's curve is based upon the assumption of monoenergetic neutrons in the center of mass system. Hence, larger values of  $\Delta E$  are to be expected because, even in the center of mass system, a spread in neutron energies is present due to proton energy spread and target thickness.

Comparison of calculated values with experimental values in Table VII makes  $J = 3$  more plausible than  $J = 2$ . While the cross sections obtained with each sample thickness can be made to fit experimental values (with judicious choices of  $\Delta E$ ) for both  $J$  values, it is to be noted that the calculated change in cross sections for different target thicknesses is more consistent with experimental values for  $J = 3$  than for  $J = 2$ . Also, cross sections obtained from the difference method are considerably more consistent for  $J = 3$ . Accordingly,  $J = 3$ , is favored over  $J = 2$  on the basis of this system of analysis.

In conclusion, the value  $J = 3$  with a width,  $\Gamma$ , of 0.76 kev seems to be the value most consistent with all data. The





value  $J = 2$  with a width,  $\Gamma$ , of 1.03 kev cannot be ruled out, however.  $J = 0$  and  $J = 1$  are inconsistent in that experimental cross section values exceed the theoretical values for such quantum numbers.  $J = 3$  is more consistent than  $J = 2$  in peak height analyses based upon both Gaussian and rectangular neutron energy distributions, as shown in Tables VI and VII.

An assignment of  $J = 3$  for this level is also indicated by the differential cross section measurements of R. C. Block (11).



## Chapter VII

### THE FLUORINE RESONANCES AT 27 KEV, 49 KEV, AND 100 KEV

Analyses were made of the 27 kev, the 49 kev, and the 100 kev resonances of fluorine by the difference method and the Gaussian resolution peak height analysis method described in Chapter III, and also by the rectangular resolution method described in Chapter VI. Patterson has shown that  $J$  is equal to or less than 2 for each of these resonances (10). Two teflon ( $C_2F_4$ ) samples were used in these experiments--one of 1/8 inch in thickness corresponding to  $1.06 \times 10^{22}$  atoms of fluorine per square centimeter, and one of 1/4 inch in thickness corresponding to  $3.32 \times 10^{22}$  fluorine atoms per square centimeter. Each of these samples has half as many carbon atoms as fluorine atoms. The minimum value of the bismuth transmission ratio curve at 12 kev was found to be 0.51 for the lithium target. Potential scattering cross sections of 3.4 barns for fluorine and 4.6 barns for carbon were assumed in evaluating these resonances.

Table VIII lists the possible theoretical peak values of the cross sections due to resonance terms alone for  $J$  values of 0, 1 and 2 for each of these three resonances.

Table IX gives the results of a Gaussian peak height





Table VIII. POSSIBLE THEORETICAL PEAK RESONANCE CROSS SECTION VALUES FOR THE 27 KEV, THE 49 KEV, AND THE 100 KEV FLUORINE RESONANCES.

$E_0$ kev	$\sigma_0$ barns $J = 0$	$\sigma_0$ barns $J = 1$	$\sigma_0$ barns $J = 2$
27	24.5	73.4	122.3
49	13.6	40.8	66.1
100	6.7	20.0	33.3

Table II. PEAK HEIGHT ANALYSIS OF THE 27 KEV FLUORINE RESONANCE, GAUSSIAN DISTRIBUTION

Teflon thickness	$A_0$	$A_1$	$A_2$
1/8 in	3	0.29	0.16
1/4 in	1.0	0.26	0.17
Average value of $y$ for both thicknesses, kev		0.55	0.61

\*  $A = \Gamma/2.83y$  where  $y$  is standard deviation of neutron energy distribution.

Subscripts correspond to  $J$  quantum numbers.

Consistency of  $A$  values for different sample thicknesses is evidence of correct  $J$  value.

Average  $y$  values based on  $\Gamma_1 = 0.40$  and  $\Gamma_2 = 0.29$  kev.



analysis of the 27 kev fluorine resonance. The value  $J = 2$  seems most consistent since  $\Delta E$  is most consistent for the two thicknesses.  $J = 1$  remains as a definite possibility.  $J = 0$  is definitely eliminated as a possibility. Widths were obtained from the findings of Patterson (10).

Table I shows the results of a rectangular resolution peak height analysis of the 27 kev fluorine resonance. The  $\Delta E$  used was 1.33 kev, compared to 1.46 obtained from Gibbon's curve (4).  $J = 2$  seems more consistent than  $J = 1$  on the basis of this

Table I. PEAK HEIGHT ANALYSIS OF THE 27 KEV FLUORINE RESONANCE BASED UPON A RECTANGULAR NEUTRON ENERGY DISTRIBUTION

Sample	$\sigma_0$ experimental	$\sigma_0$ for $J = 1$	$\sigma_0$ for $J = 2$
Both, diff. meth.	$55.9 \pm 1.5$	29.3	52.0
1/8 inch teflon	24.8	23.7	26.8
1/4 inch teflon	19.4	22.4	23.4

All values of  $\sigma_0$  are peak values due to the resonance term alone.

$\Delta E$  obtained from Gibbon's curve (4) is 1.33 kev. Analysis based upon widths  $\Gamma = 0.40$  kev for  $J = 1$ , and  $\Gamma = 0.29$  for  $J = 2$  as determined by Patterson (10).





analysis. The theoretical values obtained should be the highest possible values that could be obtained experimentally, since they are based upon monoenergetic neutrons in the center of mass system. Two out of three of the values obtained experimentally exceed the values predicted upon the basis of  $J = 1$ . The experimental value obtained by the difference method exceeds its theoretical counterpart for  $J = 1$  by a considerable amount, but agrees fairly closely with the corresponding value for  $J = 2$ . Hence the value  $J = 2$  seems more plausible than  $J = 1$  from this method of analysis.

Table XI gives the results of a Gaussian peak height analysis of the 49 kev resonance. The value  $J = 0$  was not considered since  $\sigma_{app}$  exceeded the theoretical value of 13.6 barns for  $J = 0$ . Widths used in this analysis were those determined by Patterson (10) by area analysis. No definite conclusions can be drawn from this analysis.

An analysis based upon a rectangular resolution was made of the 49 kev resonance in order to choose between  $J = 1$  and  $J = 3$ . Table III shows the results of this analysis. The amount of the energy spread obtained from Gibbon's curve (4),  $\Delta E = 2$  kev, and higher values of  $\Delta E$  were used. Theoretical peak cross section values computed on the bases of  $J = 1$  and  $J = 2$  agree with values obtained experimentally with more or less equal consistency. Accordingly, no choice between  $J = 1$  and  $J = 2$  can be made on the basis of this analysis.





Table XI. PEAK HEIGHT ANALYSIS OF THE 49 KEV FLUORINE RESONANCE,\* GAUSSIAN DISTRIBUTION

Teflon thickness	$A_1$	$A_2$
1/8 in	0.63	0.31
1/4 in	0.60	0.34
Average value of $y$ for both thicknesses, kev	0.82	1.10

\*  $A = \Gamma/2.83 y$  where  $y$  is standard deviation of neutron energy distribution.

Subscripts correspond to  $J$  quantum numbers.

Consistency of  $A$  values for different sample thicknesses is evidence of correct  $J$  value.

Average  $y$  values based on  $\Gamma_1 = 1.42$  and  $\Gamma_2 = 0.97$  kev.

Table XII. PEAK HEIGHT ANALYSIS OF THE 49 KEV FLUORINE RESONANCE BASED UPON A RECTANGULAR NEUTRON ENERGY DISTRIBUTION

Sample	$\sigma_0$ exp.	$\sigma_0$ for $J=1, \Delta E=2$	$\sigma_0$ for $J=1, \Delta E=2.8$	$\sigma_0$ for $J=2, \Delta E=2$	$\sigma_0$ for $J=2, \Delta E=3$
Both, diff. method	$37.2 \pm 1.2$	39.5	26.0	47.5	43.5
1/8 in teflon	24.4	27.1	21.5	35.0	25.9
1/4 in teflon	22.4	26.5	20.5	30.8	22.1

\* All values of  $\sigma_0$  are peak values due to the resonance term alone.

$\Delta E$  obtained from Gibson's curve (4) is 2 kev.

Analysis based upon widths  $\Gamma = 1.42$  kev for  $J = 1$ , and  $\Gamma = 0.97$  for  $J = 2$  as determined by Patterson (10).



Table IIII shows the results of a Gaussian peak height analysis of the 100 kev fluorine resonance. The value  $J = 0$  was not considered, since  $\sigma_{app}$  exceeded 6.7 barns, the theoretical value corresponding to  $J = 0$ . The value  $J = 3$  was also considered as a test of the method. Of the three  $J$  values shown,  $J = 2$  seems most consistent from this method of analysis. The widths were obtained from the thesis of Dr. J.M. Patterson (10).

A rectangular neutron energy distribution is more likely than a Gaussian distribution at 100 kev. Accordingly, a rectangular distribution peak height analysis was made of this resonance. This analysis yielded strikingly good results which

Table IIII. PEAK HEIGHT ANALYSIS OF THE 100 KEV FLUORINE RESONANCE,\* GAUSSIAN DISTRIBUTION

Teflon thickness	$A_1$	$A_2$	$A_3$
1/8 in	1.65	0.51	0.33
1/4 in	1.90	0.55	0.37
Average value of $\gamma$ for both thicknesses, kev	2.0	3.3	

\*  $A = \Gamma/2.83 \gamma$  where  $\gamma$  is standard deviation of neutron energy distribution.

Subscripts correspond to  $J$  quantum numbers.

Consistency of  $A$  values for different sample thicknesses is evidence of correct  $J$  value.

Average  $\gamma$  values based on  $\Gamma_1 = 10$  and  $\Gamma_2 = 5$  kev.







gave strong evidence that  $J = 1$  is the correct angular momentum quantum number. Table XIV shows the results of this analysis. Experimental values agreed very well with those computed on the basis of  $J = 1$ .

Table XIV. PEAK HEIGHT ANALYSIS OF THE 100 KEV FLUORINE RESONANCE BASED UPON A RECTANGULAR NEUTRON ENERGY DISTRIBUTION\*

Sample	$\sigma_0$ exp.	$\sigma_0$ for $J = 1$	$\sigma_0$ for $J = 2$
Both diff. method	$14.7 \pm 1.0$	14.0	30.8
1/8 in teflon	17.7	18.6	30.8
1/4 in teflon	17.7	19.4	30.8

\* All values of  $\sigma_0$  are peak values due to the resonance term alone.

$\Delta E$  obtained from Gibbon's curve (4) was 3.33 kev.

Analysis based upon widths  $\Gamma = 10$  kev for  $J = 1$  and  $\Gamma = 5$  kev for  $J = 2$  as determined by Patterson (10).

A summary of the results of experimental analysis of the 27 kev, 49 kev, and 100 kev resonances of fluorine is given in Table XV.



Table IV. SUMMARY OF THE 27, 49, AND 100 KEV  
RESONANCES OF FLUORINE\*

Resonant energy, $E_0$ , kev	$\sigma_0$ exp barns, limits	J Assumed	$\sigma_0$ Theoret- ical	Remarks
27	58.9	0	24.5	$\sigma_0$ exp too high.
	141	1	73.4	Consistent.
		2	122.3	Most consistent.
49	37.2	0	13.6	$\sigma_0$ exp too high.
	73	1	40.8	Consistent.
		2	68.7	Consistent.
100	17.7	0	6.7	$\sigma_0$ exp too high.
	39.2	1	20.0	Most consistent.
		2	33.3	Feasible, improbable.

\*Upper limits of  $\sigma_0$  exp determined from self-absorption curve of Bethe.

Lower limits of  $\sigma_0$  exp are highest experimental values observed.

In conclusion, the value  $J = 2$  seems most consistent for the 27 kev fluorine resonance.  $J = 0$  is ruled out for this resonance because experimental values of the cross section exceed the theoretical value. Peak height analysis based upon a Gaussian neutron energy distribution favors  $J = 2$  slightly over  $J = 1$ . Peak height analysis based upon a rectangular resolution favors  $J = 2$  over  $J = 1$  somewhat more strongly. Accordingly,  $J = 2$  seems the most probable value.

In the case of the 49 kev fluorine resonance, the assignment of  $J = 1$  or  $J = 2$  seem equally justifiable. The value  $J = 0$  is



ruled out, since experimental cross sections exceed the corresponding theoretical value.

The assignment of total angular quantum number  $J = 1$  is most consistent for the 100 kev fluorine resonance based upon all methods of analysis except the Gaussian peak height analysis. Even in that case,  $J = 1$  is feasible.





APPENDIX

1. [Faint text]
2. [Faint text]
3. [Faint text]
4. [Faint text]
5. [Faint text]
6. [Faint text]
7. [Faint text]
8. [Faint text]
9. [Faint text]
10. [Faint text]

BIBLIOGRAPHY

1. [Faint text]
2. [Faint text]
3. [Faint text]
4. [Faint text]
5. [Faint text]
6. [Faint text]
7. [Faint text]
8. [Faint text]
9. [Faint text]
10. [Faint text]



## BIBLIOGRAPHY

1. Blatt, John M., and Weisskopf, Victor F., "Theoretical Nuclear Physics," John Wiley & Son, Inc., 317 (1952).
2. Breit, G., and Wigner, E. P., Physical Review, 49, 519, 642 (1936).
3. Feshbach, H., Porter, C. E., and Weisskopf, V. F., Physical Review, 96, 448 (1954).
4. Gibbons, J. M., Ph.D. Thesis, Duke University (1954).
5. Merzbacher, E. and Chern, B., "Analysis of Neutron Transmission Experiments," unpublished (1954).
6. Hibdon, Muelhouse, Selove, & Woolf, Physical Review, 77, 730 (1950).
7. "Neutron Cross Sections," Atomic Energy Commission Report AECU-2040, U. S. Government Printing Office, Washington, D. C. (1955).
8. Bethe, H. A., Reviews of Modern Physics, 9, 69 (1937).
9. Teichmann, T., Physical Review, 77, 506 (1950).
10. Patterson, J. A., Ph.D. Thesis, Duke University (1954).
11. Block, R. C., Ph.D. Thesis, Duke University (1955).













MR 21 56  
MY 12 57

DISPLAY  
5157

Thesis  
C923

29812

Crutchfield  
Interpretation of various  
nuclear resonances.

MR 21 56  
MY 12 57

DISPLAY  
5157

Thesis  
C923

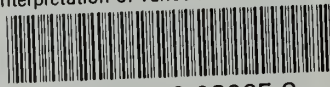
29812

Crutchfield  
Interpretation of various  
nuclear resonances.



thesC923

Interpretation of various nuclear resonances



3 2768 002 08965 8  
DUDLEY KNOX LIBRARY